Original Article

Institution of MECHANICAL ENGINEERS

Journal of AUTOMOBILE ENGINEERING

Proc IMechE Part D:
J Automobile Engineering
1–11

DOI: 10.1177/0954407014556117
pid.sagepub.com
SAGE

Detecting the combustion phase and the biodiesel blend using a knock sensor

Xuefei Chen[1], Ibrahim Haskara[2], Yueyun Wang[2] and Guoming Zhu[1]

Abstract

Existing methods of detecting the combustion phase of a diesel engine are mainly based upon high-cost in-cylinder pressure sensors. This paper presents a method of estimating the location of 75% of the mass fraction burned by using the traditional knock sensor signal. It is observed through experimental data that the knock signal has a close correlation to the location of 75% of the mass fraction burned. In this study, the knock integration is used to represent the knock intensity, while the piecewise knock integration (integration over a crank angle of 1°) is used to detect the location of 75% of the mass fraction burned. The proposed estimation method was validated using the experimental data and provided an accurate estimation of the location of 75% of the mass fraction burned. In addition, the feasibility of using the knock sensor signal to detect the biodiesel content is demonstrated using experimental data.

Keywords

Diesel engine combustion, diesel engine performance, engine modeling, engine simulations, engine testing, engine combustion

Date received: 28 April 2014; accepted: 17 September 2014

Introduction

Detecting the combustion phase of a diesel engine is of great interest to researchers, since it can be used as the feedback signal for closed-loop combustion control to improve the fuel efficiency and to reduce the exhaust emissions of a diesel engine. In particular, the estimation of the start of combustion (SOC), which occurs shortly after the fuel injection, has attracted the most attention. The techniques that can be used to estimate the SOC in a diesel engine include using a high-speed camera to obtain the first appearance of the visible flame, and measuring the sudden rise in the in-cylinder pressure or temperature caused by combustion.[1–4] However, these detection technologies can be used only in the laboratory environment because of the high cost and the low sensor durability.

Over the past few decades, numerous efforts have been devoted to developing numerical models of the ignition delay, defined as the time interval between the start of injection and the SOC. The combustion ignition delay consists of a physical delay and a chemical delay. The physical delay includes the time required for fuel atomization, vaporization, and mixing with the air, whereas the chemical delay consists of the processes of pre-combustion reactions of the fuel, air, and residual gas mixture which lead to autoignition.[1] In general, these numerical ignition delay models were developed as a function of the mixture pressure, the temperature, and the composition,[4–9] and the most commonly used model is based upon the Arrhenius function similar to that proposed by Wolfer[5] according to

$$\tau_{id} = AP^{-n}\exp\left(\frac{E_a}{R_u T}\right) \quad (1)$$

where P and T are the in-cylinder pressure and temperature respectively, E_a is the activation energy, R_u is the universal gas constant, and A and n are calibration parameters. However, those models showed the limited predictive ability of the ignition delay, compared with experimental results.

[1]Department of Mechanical Engineering, Michigan State University, East Lansing, Michigan, USA
[2]General Motors Company, Global Research and Development, Warren, Michigan, USA

Corresponding author:
Guoming Zhu, Department of Mechanical Engineering, Michigan State University, East Lansing, MI 48824, USA.
Email: zhug@egr.msu.edu

As a result, many studies have concentrated on finding a low-cost sensor for SOC detection and estimation. Among these, the traditional knock sensor has been considered as a promising candidate owing to its intrinsic relations between the combustion pressure wave and the vibration signals.[10] The phenomenon of the fuel–air mixture in the end gas zone which is autoignited before the arrival of the flame is called autoignition. Autoignition is the normal working principle in diesel engines. However, when autoignition happens under high-pressure high-temperature conditions, it becomes harmful and is called knock. Severe knock could cause engine damage. A knock sensor is used to measure the vibration intensity of the cylinder head or engine block, and the knock intensity, defined as the integral of the absolute knock signal over a given crank angle window (see equation (5)), is often used to measure the knock severity. Kim and Min[11] proposed the use of the wavelet transform of the engine knock signal to detect the SOC, while Jargenstedt[12] proposed an approach for detecting the SOC by using the envelope of the knock sensor signal. The knock sensor was also used as an indicator of the SOC for homogeneous charge compression ignition (HCCI) engines.[13] However, further investigation showed that the knock signal is usually very weak at the SOC owing to its low sensitivity. Therefore, Polonowski et al.[14] used a laboratory-grade accelerometer sensor for detecting the SOC.

Since the SOC is defined as the crank location when 1% fuel is burned, the actual SOC is very difficult to detect because of the early stage of the combustion. Therefore, many studies use the location of 10% of the mass fraction burned (MFB10) as the indication of the SOC.[15,16] The location of 50% of the mass fraction burned (MFB50) and the location of 90% of the mass fraction burned (MFB90) are also widely used in industry and research, and they are usually calculated using an in-cylinder pressure sensor. However, it was observed from the experimental data that the knock signal is fairly weak at the MFB10 location and the MFB50 location owing to the transport delay of the combustion vibration signal from the cylinder to the knock sensor. Instead, the knock signal has a high correlation to the location of 75% of the mass fraction burned (MFB75). On the other hand, since the difference between the MFB50 location and the MFB75 location is usually very small, the MFB75 location could be a good indicator for the combustion phase. This is the main motivation to estimate the MFB75 location using the knock signal in this paper.

Two traditional knock sensors (used on a 2012 GM Cruze) and one instrumentation accelerometer sensor (Omega ACC793) were used during the experimental study to detect the MFB75 location. This demonstrates that the sensitivity of the traditional knock sensor is sufficiently good for this application, which provides a low-cost alternative for combustion phase detection. The integration of the knock sensor signal over fixed crank angles (CAs) was used as the indicator of the knock intensity, while the difference in the knock integration over each CA was used to detect the MFB75 location. Two types of fuel, namely petroleum diesel (fuel blend with 0% biodiesel (B0)) and canola-based biodiesel (fuel blend with 100% biodiesel (B100)),[17] as well as their blend (fuel blend with 50% biodiesel (B50)), were investigated. As a result, the proposed method indicates that the MFB75 location can be detected consistently.

Besides the study of the combustion phase detection using the knock signal, the feasibility of using the knock sensor signal to identify the biodiesel content was also investigated in this study. Note that different biodiesel contents leads to different cetane numbers (CNs), which results in different combustion processes, such as different SOCs, different burn rates, and different burn durations.[18–20] Therefore, in order to optimize the combustion process for biodiesel engines, it is necessary to estimate the blend of the biodiesel in real time. The existing approaches of detecting the fuel content are based upon oxygen sensors,[21–24] in-cylinder pressure sensors,[25] ionization sensors,[26] and an ionic polymer–metal composite beam flow sensor.[27] In this paper, three fuel blends (B0, B50, and B100) were used during the combustion tests on a single-cylinder optical diesel engine. Note that canola has a higher CN than petroleum diesel does. The biodiesel content was estimated on the basis of the knock integration. The test results show a clear difference between B0 and B50, whereas the difference between B50 and B100 is not as obvious. It was also observed that the estimated MFB75 locations can be used for fuel blend estimation since the biodiesel content also affects the combustion phase.

All tests, including the high-speed combustion-imaging tests, that show the correlation between the knock signal and the combustion phase were conducted using a single-cylinder optical engine. Because of the speed limit of the optical engine, the engine speed in this study was limited to 1500 r/min. Note that the engine speed of 1500 r/min is close to the rated engine speed (1600 r/min). In future work, tests will be conducted on a single-cylinder metal engine with wide speed and load ranges, and the correlation between MFB75 and MFB50, as well as the biodiesel content detection using the combined criteria of the knock intensity integral (the estimated MFB75 location), will be investigated.

Combustion experiment setup

The engine combustion experiments were conducted using a single-cylinder optical diesel engine. The engine specifications are listed in Table 1. The intake manifold pressure and the intake air temperature were maintained at 1.35 bar and 25 °C respectively. Note that no external exhaust gas recirculation (EGR) was used in this study. The diesel injector used in the test was a Siemens piezo injector using a six-hole nozzle with holes

Table 1. Engine specifications.

Bore	95 mm
Stroke	105 mm
Displacement	0.75 l
Number of cylinders	1
Compression ratio	17:1
Direct-injection system pressure	125 MPa
Rated torque	12.72 kg m
Rated power	32 kW

of 0.185 mm diameter and a cone angle of 154°, and the fuel pressure in the common rail was regulated at 125 MPa. One laboratory-grade accelerometer sensor and one knock sensor were mounted directly on the cylinder wall as shown in Figure 1 to minimize the mechanical vibration noise introduced by the other moving parts of the engine. The other knock sensor was positioned on the cylinder head, a spot closest to the cylinder. The in-cylinder pressure signal was measured with a Kistler pressure transducer. All combustion data including knock and pressure signals were recorded with a baseline combustion analysis system (CAS) from AND Technologies, and all the signals were sampled at 60 kHz.

The tests were conducted at two engine speeds (1200 r/min and 1500 r/min), owing to the speed limit of the optical engine. The engine load was maintained at an indicated mean effective pressure of 5 bar by adjusting the fuel injection pulse width. Two types of fuel injection mode, first, only a main injection (a long injection pulse) and, second, a main injection with a pilot injection (a short fuel injection before the main injection), were used during the study. In order to study the knock sensor responses to different knock intensities, the injection timing was changed while the fuel injection pulse width was kept constant.

Diesel combustion usually consists of a cold flame phase and a blue flame phase, as well as an explosion flame phase.[28,29] However, it is difficult to distinguish between the blue flame phase and the explosion flame phase, because there exists no exact single point of the SOC.[28–30] Squib et al.[30] used the infrared and visible imaging techniques simultaneously to study the combustion process from fuel spray to the end of combustion. In this paper, high-speed combustion images were obtained through optical engine tests and were used to correlate the knock signal with the combustion phase. The high-speed camera used in this research was a Photron Fastcam APX RS. A shutter speed of 98 μs was used at a frame rate of 10,000 frames/s with a 512 × 512 pixel resolution. The frames were synchronized with the data collected using the CAS by a transistor–transistor logic trigger pulse. Figure 1 shows the diagram of the high-speed imaging test.

High-speed combustion-imaging tests

As mentioned above, the high-speed combustion-imaging tests were conducted to investigate the relationship between the knock sensor signal and the combustion phase. The combustion phase is represented by the mass fraction burned (MFB) in this paper. The MFB at the kth interval is calculated from[31,32]

$$\mathrm{MFB}_k = \frac{\sum_0^k \Delta P_c}{\sum_0^N \Delta P_c} \tag{2}$$

where ΔP_c represents the pressure rise due to combustion, which is calculated from

$$\Delta P_c = \Delta P - \Delta P_v \tag{3}$$

where ΔP is the in-cylinder pressure change, and ΔP_v represents the pressure rise due to the combustion chamber volume change, which is calculated from

$$\begin{aligned} \Delta P_v &= P_k - P_{k-1} \\ &= P_{k-1}\left[\left(\frac{V_{k-1}}{V_k}\right)^n - 1\right] \end{aligned} \tag{4}$$

where P_k is the in-cylinder pressure at the kth step.

It was observed that the knock sensor mounted on the cylinder wall provided a similar level of signal-to-noise ratio to that of the accelerometer, whereas the signal-to-noise ratio of the knock sensor installed on the cylinder head was very low. This is because the valve events inside the cylinder head introduce significant noise into the knock sensor signal. A knock sensor mounted on the cylinder wall was used in the rest of the paper, and it was filtered by a bandpass filter with cutoff frequencies of 3 kHz and 18 kHz respectively.

Figure 2 shows the combustion images synchronized with the in-cylinder pressure, the MFB, and the knock signal. Note that the dot-dashed curve represents the location of the fuel injection (active low). In this combustion case, a 0.5 ms fuel pulse was delivered at 12° CA before top dead center (BTDC). The first visible flame (a tiny orange flame with a certain blue flame) was observed at a CA of around 182°. It can be seen that this SOC was obtained by the knock sensor. The significant flame was developed around the MFB10 location. However, the knock signal did not show a

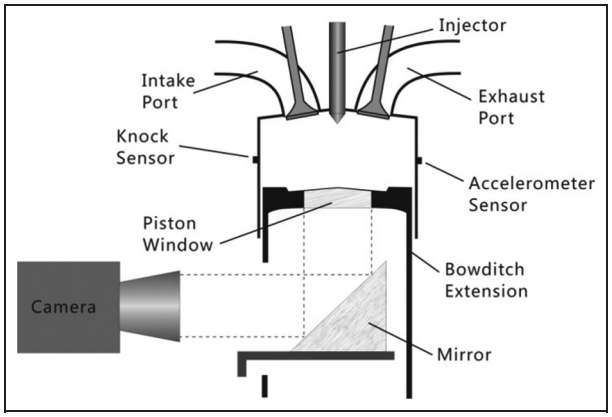

Figure 1. Optical test setup diagram.

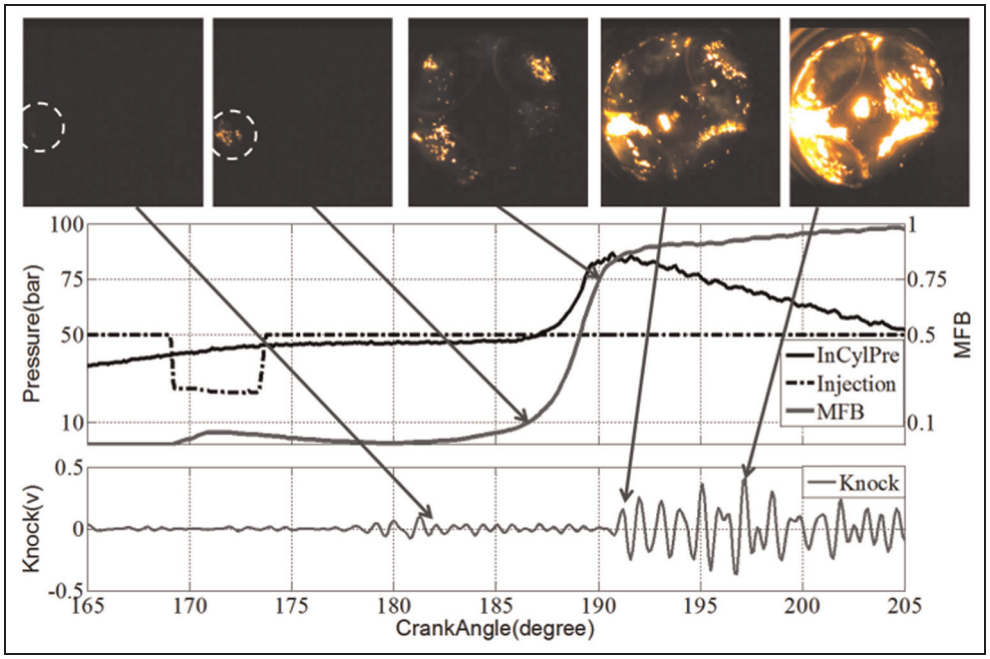

Figure 2. High-speed images with the in-cylinder pressure and knock signals.
InCylPre: in-cylinder pressure; MFB: mass fraction burned.

high signal-to-noise ratio until a CA of 191°, where the combustion phase was very close to the MFB75 location. It can be observed that the majority of the knock signal occurs between the MFB75 location and the MFB90 location.

A series of validation tests demonstrates similar correlations between the knock sensor signal and the combustion phase, as shown in Figure 2. Therefore, detection of the MFB75 location using the knock sensor signal was proposed in this paper.

MFB75 detection method

Figure 3 shows a combustion event with a relatively high knock intensity, which is evaluated on the basis of the signal KnockInt defined by

$$\text{KnockInt} = \int_{\text{TDC}}^{\text{TDC}+20} |\text{Knock}(\tau)|\, d\tau \tag{5}$$

where τ represents the CA, Knock is the filtered knock sensor signal, and KnockInt represents the knock integration over a CA window of 20° starting from top dead center. The signal KnockIntCA(i) is the integration of the knock signal over a CA of 1° starting at the ith CA. It is defined by

$$\text{KnockIntCA}(i) = \int_{i}^{i+1} |\text{Knock}(\tau)|\, d\tau \tag{6}$$

Note that KnockIntCA represents the difference in KnockInt over a CA of 1°.

In Figure 3, the rising edge of the signal MFBflag denotes the MFB10 location, and the falling edge of MFBflag denotes the MFB75 location. It can be seen that the MFB75 location is very close to the KnockIntCA peak, which is the first KnockIntCA peak greater than one. In addition, the subsequent KnockIntCA peaks are all greater than one.

The knock integration shown in Figure 3 reaches 80. A similar investigation was conducted for combustion with relatively weak knock at a light load, whose KnockInt is less than 20, as shown in Figure 4. However, the KnockIntCA peak corresponding to the point of MFB75 has similar characteristics to the case shown in Figure 3. In this case, the first KnockIntCA peak is around 0.75.

From the above observations, it is proposed to use the following criteria for detecting the MFB75 location based upon the knock signal. The MFB75 location can be determined at the ith CA if

$$\text{KnockIntCA}(i-1) \leqslant \text{KnockIntCA\_Thresh} \tag{7}$$

$$\text{KnockIntCA}(j) \geqslant \text{KnockIntCA\_Thresh with } j = i \cdots i+2 \tag{8}$$

and

$$\frac{\text{KnockIntCA}(i)}{(1/i)\sum_{j=1}^{i} \text{KnockIntCA}(j)} \geqslant \alpha \tag{9}$$

where KnockIntCA_Thresh and α are two estimation calibration parameters. Figure 5 shows the flow chart of the proposed MFB75 estimation algorithm. The physical interpretation of the detection logic is to

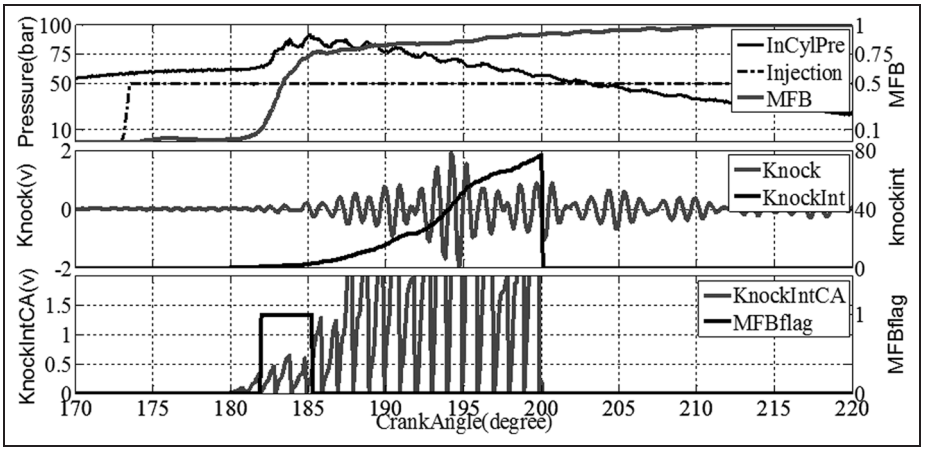

Figure 3. MFB75 detection with intense knock.
InCylPre: in-cylinder pressure; MFB: mass fraction burned: KnockInt; knock signal integration over a crank angle of 20°; KnockIntCA: knock signal integration over a crank angle of 1°; MFBflag; MFBflag indicating that the mass fraction burned is between 10% and 75%.

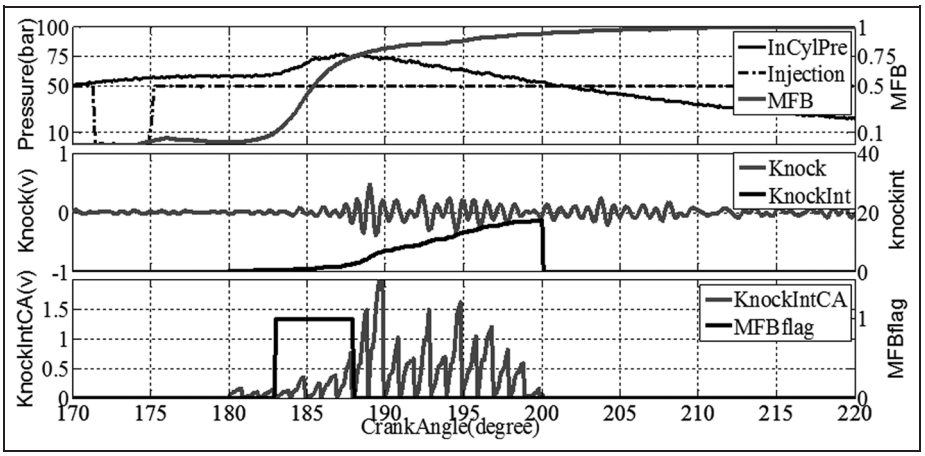

Figure 4. MFB75 detection with weak knock.
InCylPre: in-cylinder pressure; MFB: mass fraction burned: KnockInt; knock signal integration over a crank angle of 20°; KnockIntCA: knock signal integration over a crank angle of 1°; MFBflag; MFBflag flag indicating that the mass fraction burned is between 10% and 75%.

correlate the sharp increase in KnockIntCA to locate the MFB75.

Based upon the above detection strategy, statistical analysis was conducted. In this analysis, engine tests with three different fuels (B0, B50, and B100) were conducted at two engine speeds (1200 r/min and 1500 r/min). Several groups of injection parameters were tested in order to study the proposed approach for different knock intensities. For each test, the mean value of the MFB75 location and the mean absolute deviation (MAD) were calculated over 40 combustion cycles. Note that the 'mean of the pressure-based MFB75ò¥ is based upon the in-cylinder pressure sensor and the 'mean of the knock-based MFB75ò¥ is estimated using the knock intensity. In this study, KnockIntCA_Thresh was set at 0.7, and α was fixed at 1.5.

Table 2 provides the analysis results. It can be seen that the estimated mean MFB75 values based on the knock signal are very close to those calculated from the in-cylinder pressure signal. On the basis of the MAD, it can be concluded that the estimation has a good cycle-to-cycle accuracy with the largest estimation error equal to 2°. Since the knock signal-to-noise ratio

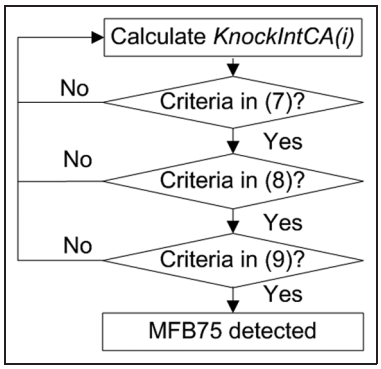

Figure 5. Working flow chart for the MFB75 estimation algorithm.
KnockIntCA: knock signal integration over a crank angle of 1°; MBF75: 75% of mass fraction burned.

Table 2. Statistical analysis of the detected MFB75 location.

Fuel	Pilot injection		Main injection		Mean of the pressure-based MFB75 (deg)	Mean of the knock-based MFB75 (deg)	Mean absolute deviation	Knock integration	Engine speed (r/min)
	Timing (deg CA)	Pulse (ms)	Timing (deg CA)	Pulse (ms)					
B0	0	0	10	0.5	10.8	10.6	2	20.3	1500
B0	0	0	13	0.5	9.9	8.8	0.9	18.4	1500
B0	24	0.35	4	0.5	12.4	11.7	0.9	24.7	1500
B0	24	0.35	4	0.5	10.5	11.5	1.2	25.8	1200
B50	0	0	10	0.5	8	8.6	0.8	50.7	1500
B50	0	0	13	0.5	6.7	6.4	0.5	51	1500
B50	24	0.25	4	0.5	12.5	13.1	1	20.8	1500
B50	24	0.35	4	0.5	10.3	10.3	0.5	42	1200
B100	0	0	10	0.5	7.1	6.4	1.3	46.5	1500
B100	0	0	13	0.5	5.3	5.1	0.5	57.7	1500
B100	24	0.35	4	0.5	11.8	11.1	1.4	27.1	1500
B100	24	0.25	4	0.5	11.7	13	1.4	19.1	1500
B100	24	0.35	4	0.45	9.6	10.8	1.3	25.9	1200

CA: crank angle; MFB75: 75% of the mass fraction burned; B0: fuel blend with 0% biodiesel; B50: fuel blend with 50% biodiesel; B100: fuel blend with 100% biodiesel.

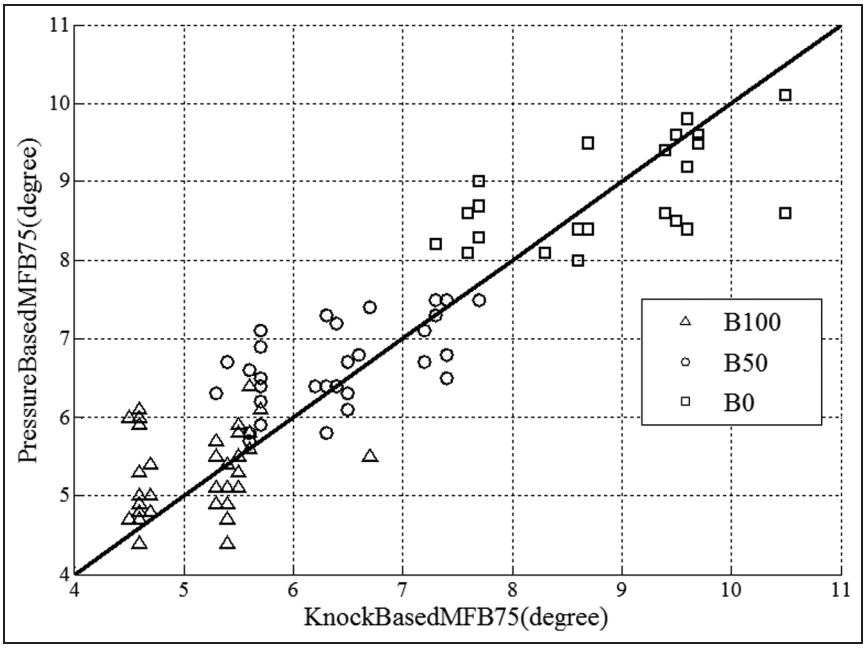

Figure 6. Correlation between the knock-based MFB75 and the pressure-based MFB75.
MBF75: 75% of mass fraction burned; B100: fuel blend with 100% biodiesel; B50: fuel blend with 50% biodiesel; B0: fuel blend with 0% biodiesel.

improves as the knock intensity (or the engine load) increases, the estimation accuracy improves as the knock intensity (or the engine load) increases. This can also be seen in Figure 6, which shows the test points of three different fuel blends with the same injection timing (13° CA BTDC) and the same injection quantity (0.5 ms fuel injection pulse width). It can be seen that the knock-based MFB75 has a fairly close correlation to the MFB75 based upon the in-cylinder pressure sensor. Figure 7 shows a comparison of the results for B50 with three different fuel injection timings (7° CA BTDC, 10° CA BTDC, and 13° CA BTDC) with the same fuel injection pulses. It can be found that the MFB75 estimation associated with the 13° CA BTDC injection provided the most accurate result. This is because injection at 13° CA BTDC led to the highest knock intensity, while injection at 7° CA BTDC led to the lowest knock intensity. It is worth pointing out that the actual MFB75 in Figure 7 is higher than the estimated MFB75 for the injection timings 7° CA BTDC and 13° CA BTDC, whereas the injection timing of 10° CA BTDC shows the opposite trend. This could be due to the variation in the correlation between the burn rate and knock sensor signal. In addition, the analysis results also show that, when the knock intensity is high, the deviation of the estimated value tends to be

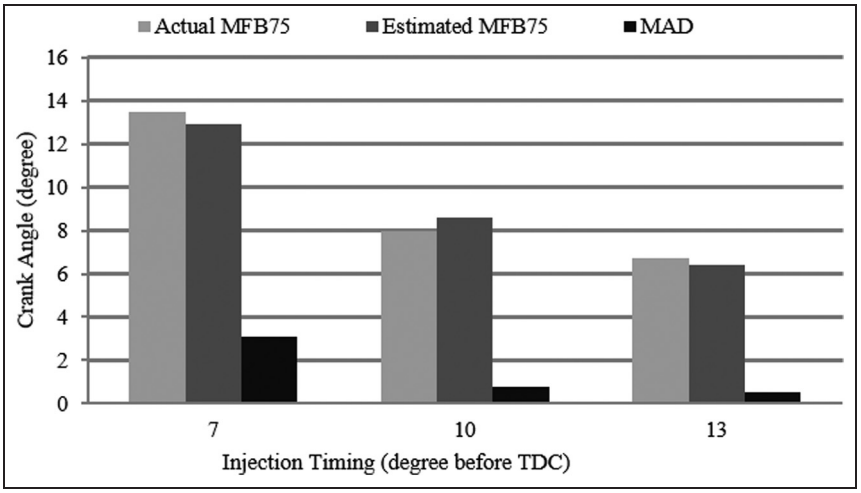

Figure 7. MFB75 estimations for the same fuel blend.
MBF75: 75% of mass fraction burned; MAD: mean absolute deviation; TDC: top dead center.

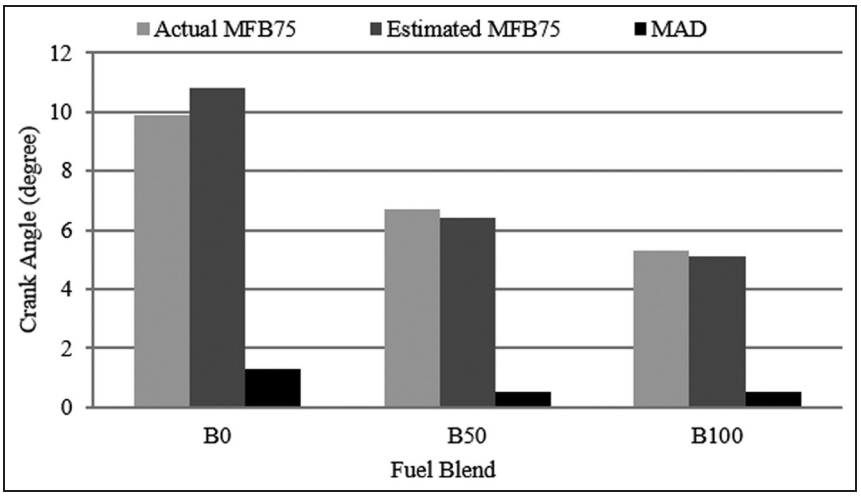

Figure 8. Comparison of MFB75 estimations for the same injection conditions.
MBF75: 75% of mass fraction burned; MAD: mean absolute deviation; B0: fuel blend with 0% biodiesel; B50: fuel blend with 50% biodiesel; B100: fuel blend with 100% biodiesel.

negative, and vice versa. This is well illustrated by Figure 8. As mentioned above, the fuel blends B50 and B100 have a higher knock tendency than does B0, which leads to earlier knock occurrence than for fuel blend B0. As a result, the estimated MFB75 locations for the fuel blends B50 and B100 tend to be earlier than the actual locations, while the estimated location for B0 tends to be later. Therefore, the absolute estimation error can be further reduced by using different KnockIntCA_Thresh and α values under different knock intensities, which, in general, are functions of the engine speed and the load conditions. The other approach is to generate an offset map as a function of the engine speed and the load. It is believed through data analysis that the estimation error can be reduced to within 1°. Since the knock intensity varies at different operational conditions for a given fuel, to detect the biodiesel blend accurately, KnockIntCA_Thresh and α can be functions of the engine operational conditions to rule out the effect of the variation in the knock intensity due to the operational conditions.

In addition, it was also noted that, for the same fuel injection conditions, the MFB75 location for B100 is the smallest, whereas that for B0 is the largest, as shown in Figure 8. This is not only because B100 starts combustion earlier, but also because it burns much faster. Therefore, it is possible that the estimated MFB75 can be used to detect the biodiesel fuel content and to optimize the combustion process. Note that, in general, the biodiesel content is unknown since diesel or biodiesel could be added into the fuel tank as required for a flexible-fuel vehicle.

Biodiesel content estimation

The interest in detecting the biodiesel content arises because the difference in the fuel contents leads to different SOCs, burn rates, burn durations, etc. This paper

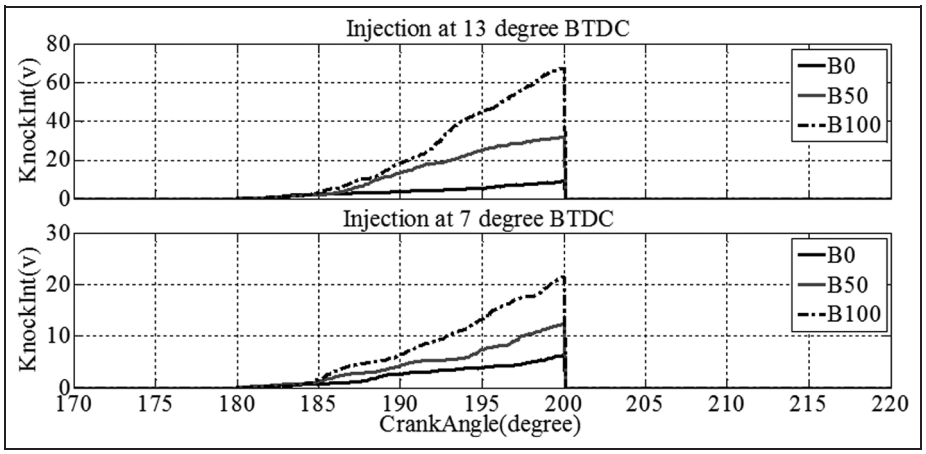

Figure 9. Knock integration without a pilot injection.
KnockInt; knock signal integration over a crank angle of 20°; BTDC: before top dead center; B0: fuel blend with 0% biodiesel; B50: fuel blend with 50% biodiesel; B100: fuel blend with 100% biodiesel.

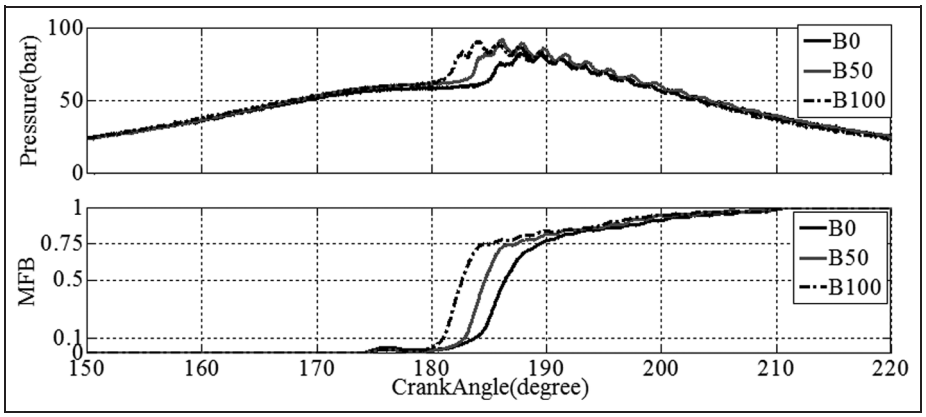

Figure 10. Comparison of the in-cylinder pressure and the MFB.
MFB: mass fraction burned; B0: fuel blend with 0% biodiesel; B50: fuel blend with 50% biodiesel; B100: fuel blend with 100% biodiesel.

studies the feasibility of using knock integration information to estimate the fuel content. Three types of fuel (B0, B50, and B100) were studied in this research.

Figure 9 shows the knock integration for the engine combustion of three different fuels under the same engine operational conditions. The same fuel pulse (0.5 ms) was used with two different injection timings (13° CA BTDC and 7° CA BTDC), which lead to different knock intensities. It can be seen that the differences between the three different fuels are quite distinct. In general, the high-CN fuel leads to low premixed phase combustion owing to a short ignition delay with smooth combustion. In this paper, a comparison was made between single-injection experiments. With little (or no) pilot injection, the combustion process in a diesel engine is similar to that in a spark ignition engine since a large amount of released energy is generated as a result of flame propagation into the gas–air mixture region.[33] With little (or no) pilot injection, the combustion could create excessive knock. During the excessive-knock operation, a high percentage of biodiesel in the fuel–air gaseous mixture induces more severe knock.[34] Therefore, B100 has the highest knock intensity in both cases, whereas B0 has the lowest, as shown in Figure 10.

Since a pilot injection reduces the knock intensity significantly, a study with a pilot injection was also conducted in this paper. The main injection is a 0.45 ms fuel pulse delivered at 4° CA BTDC. Two different pilot fuel pulses (0.2 ms and 0.3 ms) were tested with the injection timing fixed at 24° CA BTDC. Note that the engine load was close to the data shown in Figure 9. With a pilot injection, the magnitude of the knock integration is reduced dramatically, as shown in Figure 11. However, the differences in the knock intensities of the three fuels were still as distinct as in the case without a pilot injection.

Since knock is affected by many factors, such as the intake air temperature, the intake air pressure, and the injection timing, a statistical analysis was conducted by

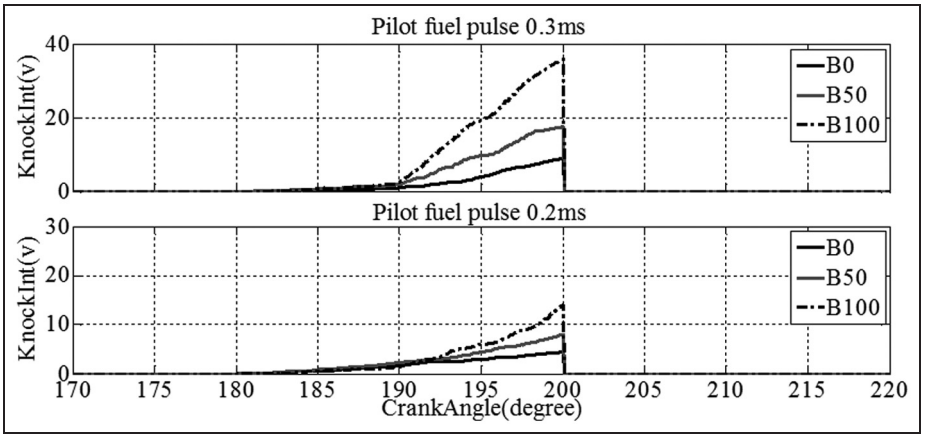

Figure 11. Knock integration with a pilot injection.
KnockInt; knock signal integration over a crank angle of 20°; B0: fuel blend with 0% biodiesel; B50: fuel blend with 50% biodiesel; B100: fuel blend with 100% biodiesel.

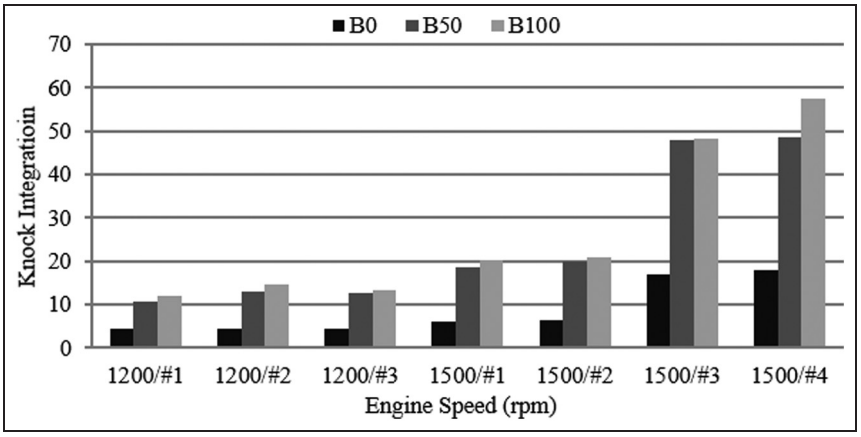

Figure 12. Comparison of the knock integration data for three fuel blends.
B0: fuel blend with 0% biodiesel; B50: fuel blend with 50% biodiesel; B100: fuel blend with 100% biodiesel; rpm: rev/min.

Table 3. Statistical analysis of knock integration.

Engine speed (r/min)	Pilot injection		Main injection		Knock integration		
	Timing (deg CA)	Pulse (ms)	Timing (deg CA)	Pulse (ms)	B0	B50	B100
1200	24	0.2	4	0.5	4.4	10.8	12.1
	24	0.3	4	0.5	4.4	13	14.8
	0	0	10	0.5	4.4	12.6	13.4
1500	24	0.2	4	0.5	6	18.5	20.2
	24	0.3	4	0.5	6.3	19.9	20.9
	0	0	10	0.5	16.9	48	48.2
	0	0	13	0.5	18.1	48.6	57.4

CA: crank angle; B0: fuel blend with 0% biodiesel; B50: fuel blend with 50% biodiesel; B100: fuel blend with 100% biodiesel.

evaluating the mean value of the knock integration over 40 consecutive combustion cycles, and the results are presented in Table 3.

The results show a clear difference between B0 and B50, whereas the difference between B50 and B100 is not that obvious except for case 4 at 1500 r/min (Figure 12). Further investigation of the fuel blend between B0 and B50 is necessary. However, the results in Figure 8 show that both the actual MFB75 location and the estimated MFB75 location have clear differences for the three fuels. Therefore, the development of an accurate biofuel estimation algorithm using both the estimated MFB75 location and the knock intensity information is very promising.

Conclusions and future work

This paper proposes a method to detect the MFB75 location using the traditional knock sensor signal. This study was motivated by using a low-cost sensor to detect or estimate the combustion phase. The experimental data show that the knock signal demonstrates a certain correlation to the MFB location. An estimation algorithm based upon the piecewise knock integral was proposed and validated using the experimental data. It shows that the MFB75 estimation error, using the knock sensor signal, is within a CA of 2°. With the help of calibrating the detecting threshold as a function of the engine speed and the load, it can be further reduced to 1° CA. In addition, an investigation into using the knock sensor signal to estimate the biodiesel blend was also conducted. The results show the feasibility of estimating the biofuel content using the knock sensor signal. Future work will be to investigate the correlation between MFB50 and MFB75 so that the estimated MFB75 information can be used in practical applications and to develop an accurate biofuel content estimation algorithm based upon both the estimated MFB75 location and the knock intensity information.

Declaration of conflict of interest

The authors declare that there is no conflict of interest.

Funding

This project was supported by General Motors under contract number GB821-NV.

References

1. Heywood JB. *Internal combustion engine fundamentals*. New York: McGraw-Hill, 1988.
2. Lee JH and Lida N. Combustion of diesel spray injected into reacting atmosphere of propane–air homogeneous mixture. *Int J Engine Res* 2001; 2(1): 69–80.
3. Aligrot C, Champoussin JC and Guerrassi N. A correlative model to predict autoignition delay of diesel fuels. SAE paper 970638, 1997.
4. Assanis DN, Filipi ZS, Fiveland SB and Syrimis M. A predictive ignition delay correlation under steady-state and transient operation of a direct injection diesel engine. *Trans ASME, J Engng Gas Turbines Power* 2003; 125: 450–457.
5. Wolfer HH. Der Zündverzug im Dieselmotor. *VDI-Forschungsheft* 1938; 392: 15–24 (transl. Ignition lag in diesel engines. Report 358, Royal Aircraft Establishment, Farnborough, Hampshire, UK, August1959).
6. Stringer FW, Clarke AE and Clarke JS. The spontaneous ignition of hybrocarbon fuels in a flowing system. *Proc. IMechE* 1969; 184(10): 212–225.
7. Henein NA and Bolt JA. Correlation of air charge temperature and ignition delay for several fuels in a diesel engine. SAE paper 690252, 1969.
8. Hardenberg HO and Hase FW. An empirical formula for computing the pressure rise delay of a fuel from its cetane number and from the relevant parameters of direct-injection diesel engines. SAE paper 790493, 1979.
9. Itoh Y and Henein NA. Determination of ignition delay in diesel engines from constant volume vessels data. In: *Spring technical conference of ASME Internal Combustion Engine Division*, Fort Collins, Colorado, USA, 27–30 April 1997, USICE-Vol. 28-1, pp. 29–34. New York: ASME.
10. Barton RK, Lestz SS and Duke LC. Knock intensity as a function of engine rate of pressure change. SAE paper 700061, 1970.
11. Kim S and Min K. Detection of combustion start in the controlled auto ignition engine by wavelet transform of the engine block vibration signal. *Measmt Sci Technol* 2008; 19: 085407.
12. Jargenstedt M. *Detection of the start of combustion using knock sensor signals*. Master's Thesis, Linköping University, Linköping, Sweden, 2000.
13. Chauvin J, Grondin O, Nguyen E and Guillemin F. Real-time combustion parameters estimation for HCCI-diesel engine based on knock sensor measurement. In: *17th IFAC world congress*, Seoul, Republic of Korea, 6–11 July, 2008, pp. 8501–8507. Laxenburg: IFAC.
14. Polonowski C, Mathur V, Naber J and Blough J. Accelerometer based sensing of combustion in a high speed HPCR diesel engine. SAE paper 2006-01-0972, 2006.
15. Dec JE. Advanced compression-ignition engines – understanding the in-cylinder process. *Proc Combust Inst* 2009; 32(2): 2727–2742.
16. Attebery AD. *Investigating the effects of internally trapped residuals on the performance of homogeneous charge compression ignition (HCCI) engine*. MS Thesis, Missouri University of Science and Technology, Rolla, Missouri, USA, 2012.
17. Demirbas A. Importance of biodiesel as transportation fuel. *Energy Policy* 2007; 35: 4661–4670.
18. Szybist J, Song J, Alam M and Boeham A. Biodiesel combustion, emission and emission control. *Fuel Processing Technol* 2007; 88: 676–691.
19. McCrady J, Hansen A and Lee C. Modeling biodiesel combustion using GT-Power. In: *2007 ASAE annual meeting*, Chicago, Illinois, USA, 11–14 August 2007, paper 076095. St Joseph, Michigan: ASABE.
20. McCrady J, Hansen A and Lee C. Combustion and emissions modeling of biodiesel using GT-Power. In: *2008 ASAE annual meeting*, Providence, Rhode Island, USA, 29 June–2 July 2008, paper 084045. St Joseph, Michigan: ASABE.
21. Snyder D, Adi G, Bunce M, et al. Steady-state biodiesel blend estimation via a wideband oxygen sensor. *Trans ASME, J Dynamic Systems, Measmt Control* 2009; 131(4): 988–993.
22. Snyder D, Adi G, Bunce M, et al. Dynamic exhaust oxygen based biodiesel blend estimation with an extended Kalman filter. In: *2010 American control conference*, Baltimore, Maryland, USA, 30 June–2 July 2010, pp. 3009–3014. New York: IEEE.
23. Ahn K, Stefanopoulou A and Jankovic M. Estimation of ethanol content in flex-fuel vehicles using an exhaust gas oxygen sensor: model, tuning and sensitivity. In: *ASME 2008 dynamic systems and control conference*, Ann Arbor, Michigan, USA, 20–22 October 2008, paper DSCC2008-2232, pp. 947–954. New York: ASME.

24. Chen X, Wang Y, Haskara I and Zhu G. Air-to-fuel ratio control with adaptive estimation of biofuel content for diesel engine LNT regeneration. In: *2012 American control conference*, Montreal, Quebec, Canada, 27–29 June 2012, pp. 4957–4962. New York: IEEE.
25. Ahn K, Stefanopoulous A, Jiang L and Yilmaz H. Ethanol content estimation in flex fuel direct injection engines using in-cylinder pressure measurements. SAE paper 2010-01-0166, 2010.
26. Daniels C, Zhu G, Mammen W and Zhang M. Virtual flex fuel sensor for spark ignition engines using ionization signal. US Patent 7921704B2, 12April2011.
27. Chen X, Zhu G, Yang X et al. Model-based estimation of flow characteristics using an ionic polymer–metal composite beam. *IEEE/ASME Trans Mechatronics* 2013; 18(3): 932–943.
28. Pickett L, Kook S and Williams T. Visualization of diesel spray penetration, cool flame, ignition, high temperature combustion, and soot formation using high-speed imaging. SAE paper 2009-01-0658, 2009.
29. Katrasnik T, Trenc F and Opresnik S. A new criterion to determine the start of combustion in diesel engines. *Trans ASME, J Engng Gas Turbines Power* 2006; 128: 928–933.
30. Squib C, Schock H, Stuecken T et al. A development of simultaneous infrared and visible imaging techniques with pressure data in an optically accessible diesel engine operating at part load with high EGR. SAE paper 2011-01-1395, 2011.
31. Mittal M, Zhu G and Schock H. Fast mass-fraction-burned calculation using the net pressure method for real-time applications. *Proc IMechE Part D: J Automobile Engineering* 2009; 223(3): 389–394.
32. Brunt MFJ and Emtage AL. Evaluation of burn rate routines and analysis errors. SAE paper 970037, 1997.
33. Saidi M, Far K and Pirouzanah V. Analysis of combustion process in dual fuel diesel engine: knock phenomenon approach. SAE paper 2005-01-1132, 2005.
34. Lowe D, Lin T, Wu W and Tan A. Diesel knock combustion and its detection using acoustic emission. *J Acoust Emission* 2011; 29: 78–88.

Appendix 1

Abbreviations

BTDC	before top dead center
B0	fuel blend with 0% biodiesel
B50	fuel blend with 50% biodiesel
B100	fuel blend with 100% biodiesel
CA	crank angle
CN	cetane number
EGR	exhaust gas recirculation
HCCI	homogeneous charge compression ignition
KnockInt	knock signal integration over a crank angle of 20°
KnockIntCA	knock signal integration over a crank angle of 1°
MAD	mean absolute deviation
MFB	mass fraction burned
MFBflag	flag indicating that the mass fraction burned is between 10% and 75%
MFB10	10% of the mass fraction burned
MFB50	50% of the mass fraction burned
MFB75	75% of the mass fraction burned
MFB90	90% of the mass fraction burned
SOC	start of combustion